Supporting Information

Photoactivated Chiral Molecular Clamp Rotated by Selective Anion Binding

Yiping Liu, Aiyou Hao and Pengyao Xing*

School of Chemistry and Chemical Engineering, Shandong University, Jinan 250100, People's Republic of China.

Email: xingpengyao@sdu.edu.cn

Table of Contents

I. Experimental details

Materials

All solvents were reagent grade without further purification. Dimethylsulfoxide (DMSO), Acetonitrile (CH_3CN), Methanol (CH_3OH), pyridine, Methylcyclohexane (MCH) and Tetrahydrofuran (THF) were purchased from Jinan Saibo Instrument Co., Ltd.

1,8-Diazabicyclo[5,4,0]undec-7-ene (DBU), 4-(Cyanomethyl)benzoic acid, 1-Naphthaldehyde, 1-(3-Dimethylaminopropyl)-3-ethylcarbodiimide (EDC), 4-Dimethylaminopyridine (DMAP), 1-Hydroxybenzotrizole (HOBT), (1R,2R)-Diphenylethane-1,2-diamine, (1S,2S)-Diphenylethane-1,2-diamine, 1R,2R-Diaminocyclohexane, 1S,2S-Diaminocyclohexane, Tetrabutylammonium fluoride (1M in THF), Tetrabutylammonium chloride, Tetrabutylammonium bromide, Tetrabutylammonium iodide and Tetrabutylammonium nitrate were purchased from Shanghai Bidepharm and used as received.

Instrumentation

^{1}H NMR spectra, ^{13}C NMR spectra were obtained by BRUKER AVANCE III HD 400.

High-Resolution Mass Spectra (HR-MS) were performed on an Agilent Q-TOF 6510. Circular dichroism (CD), temperature-variable CD were measured with an Applied Photophysics ChirascanV100 model. UV-Visible absorption spectra at room temperature were recorded on a UV-1900 Shimadzu spectrophotometer. Fluorescence spectra was made on a RF 6000 Shimadzu fluorophotometer. Scanning electron microscope (SEM) images were measured by a Zeiss scanning electron microscope (Germany). The samples for SEM detection were dropped in the silicon pellet, dried and then sprayed by the platinum before detection. The statistics of particle size distribution was carried out by the combination of SEM images and Image J. Circularly polarized luminescence (CPL) were acquired by JASCO CPL 300.

Sample preparation

The compounds were pre-dissolved in tetrahydrofuran (THF) for preparing

concentrated solutions (0.01 M) under ultrasonic dissolution. Then, a series of 100 uL concentrated solutions were transferred into vials, followed by drying them in a vacuum drying oven. The samples have been completely dried and cooled for the next steps. Meanwhile, concentrated solutions (1 mM) of TBAX (X = F^-, Cl^-, Br^-, I^- and NO_3^-) were prepared and added to the systems with different equivalent ratios. Finally, the volume of THF required was calculated and THF was added to the solution with a total volume of 1ml, and thus solution samples of 1×10^{-3} M with different ratios of anions were obtained, respectively. In addition, the assemblies for SEM samples were prepared in mixed solvents with THF: MCH=1:9. The absolute quantum yields of the photoisomerization in this system were measured by the integrating sphere method using FLS920.

II. Supplementary Data

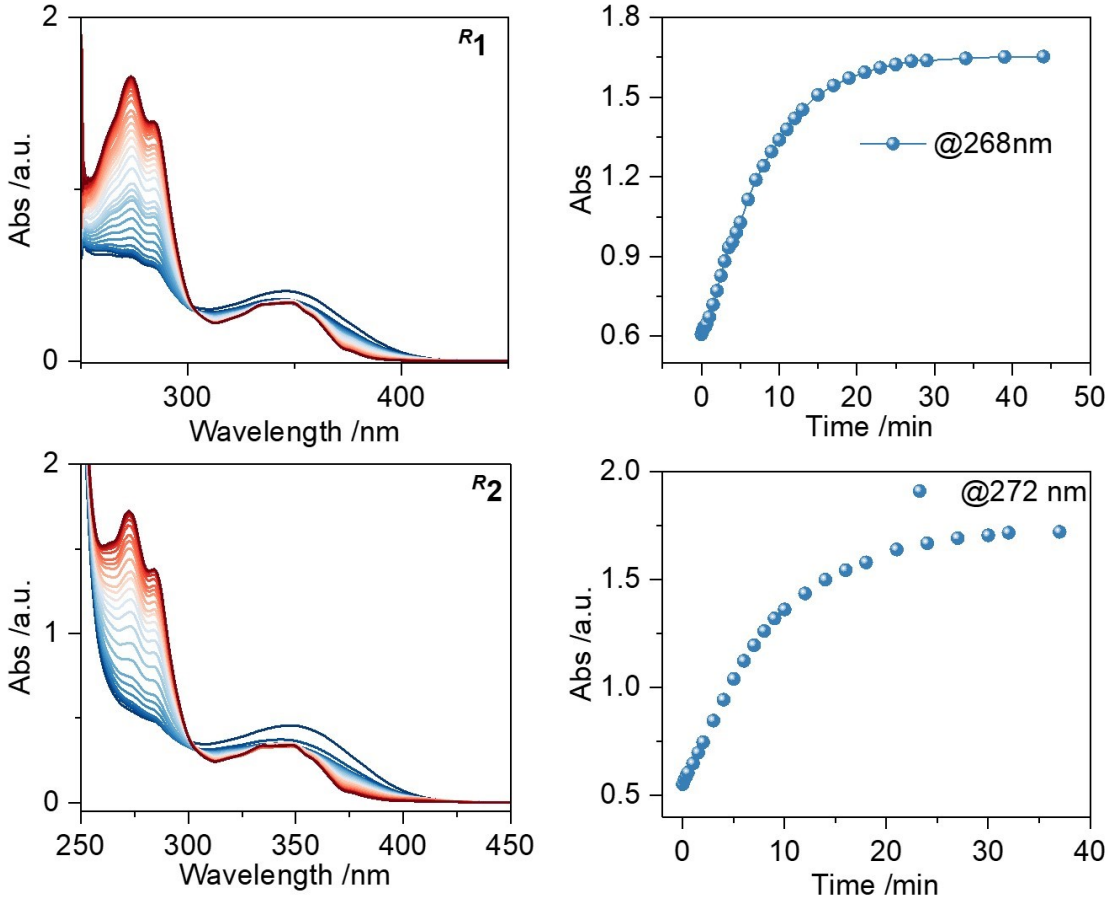

Figure S1. Absorption spectra along with the 365 nm photo irradiation of ***R*1** and ***R*2** in

DMSO (0.1 mM).

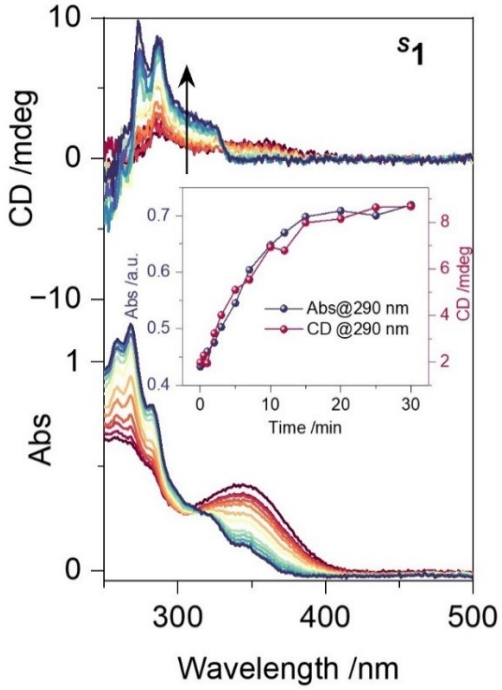

Figure S2. CD spectra of compound ^{S}**1** registered in THF (0.1 mM). The built-in image is Cotton effect intensity at 290 nm of ^{S}**1** as a function of photo irradiation time.

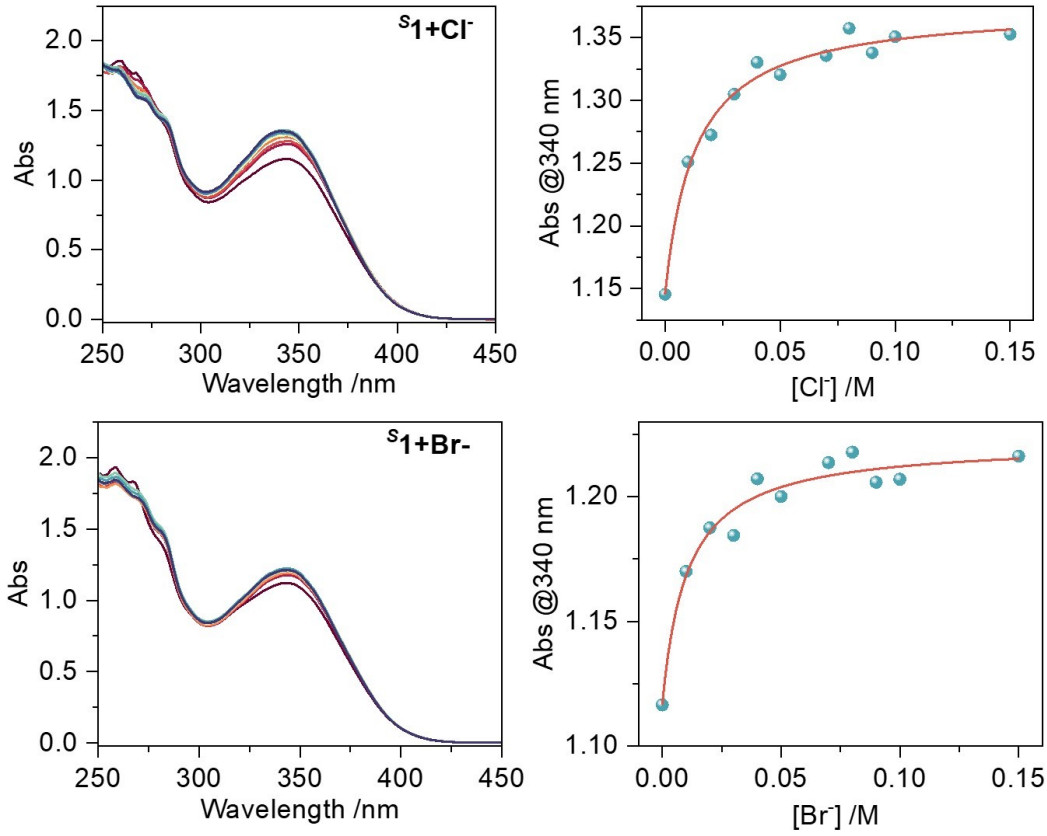

Figure S3. Absorption titration studies and the 1:1 fitted curve of ^{S}**1** (0.05 mM in

THF) and Cl^- /Br^-.

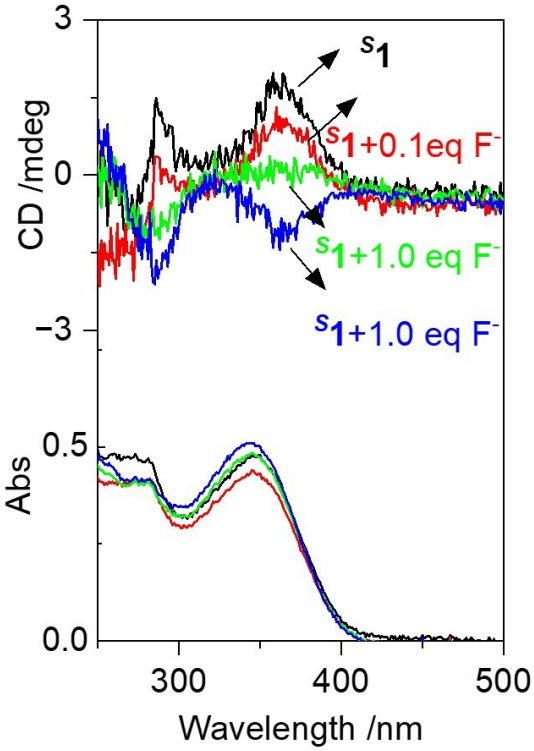

Figure S4. CD spectra changes of ***S*1** (0.1 mM in THF) with increasing molar equiv. of F^-.

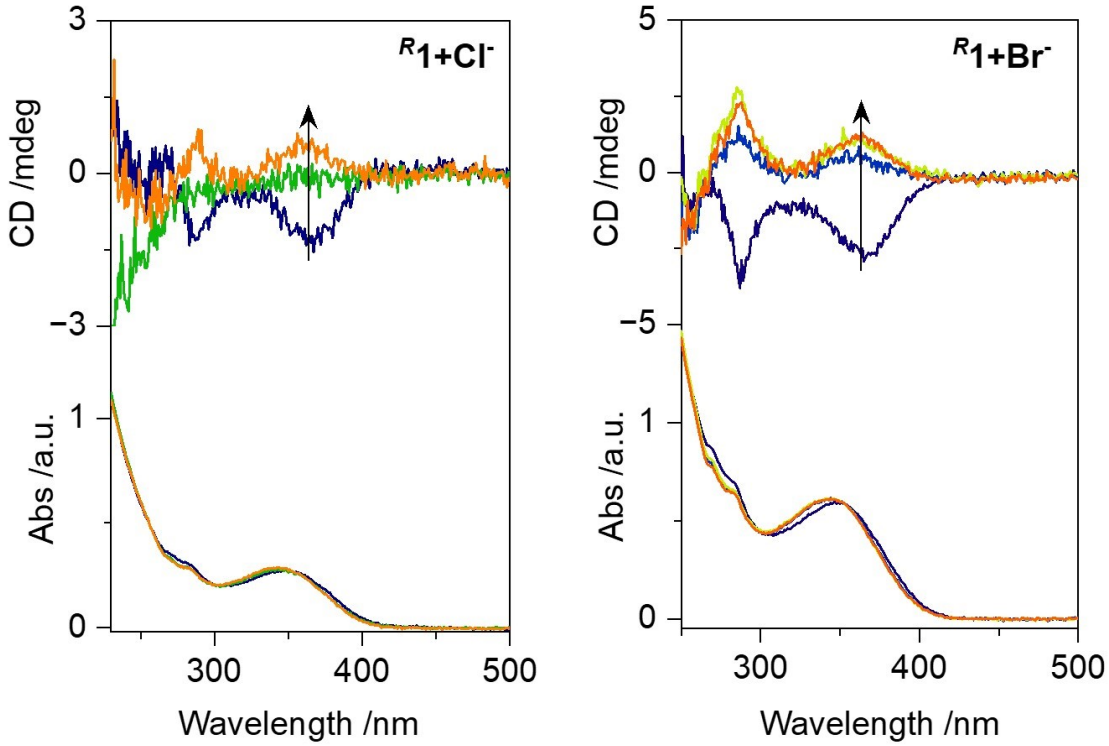

Figure S5. CD spectra changes of ***R*1** (0.1 mM in THF) with increasing molar equiv.

of Cl^- and Br^-, respectively.

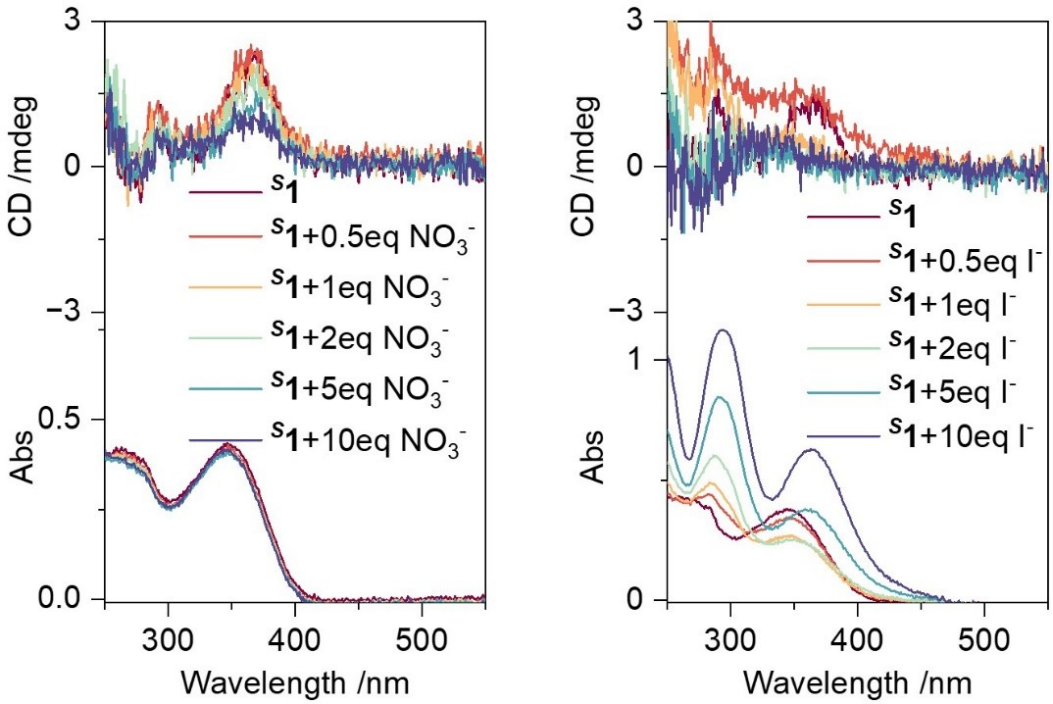

Figure S6. CD spectra changes of ^{S}**1** (0.1 mM in THF) with increasing molar equiv. of NO^{3-} and I^-, respectively.

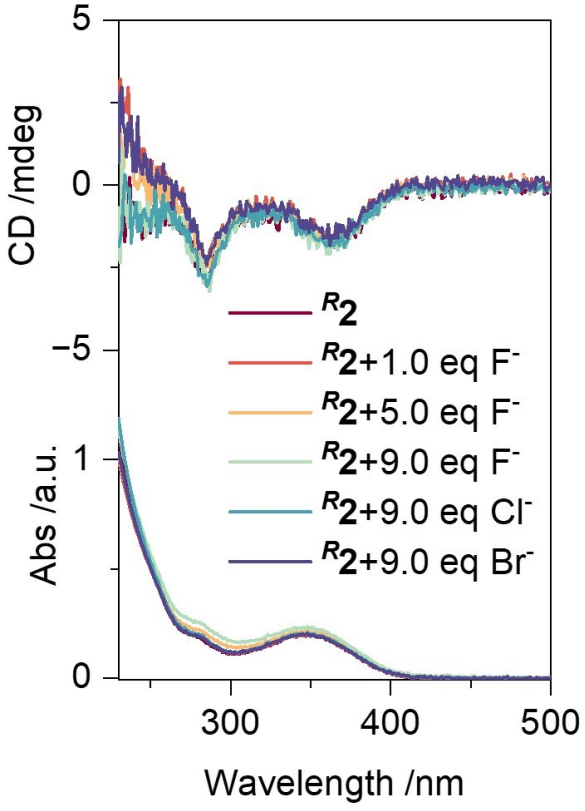

Figure S7. CD spectra changes of ^{R}**2** (0.1 mM in THF) with increasing molar equiv. of F^-, Cl^- and Br^-, respectively.

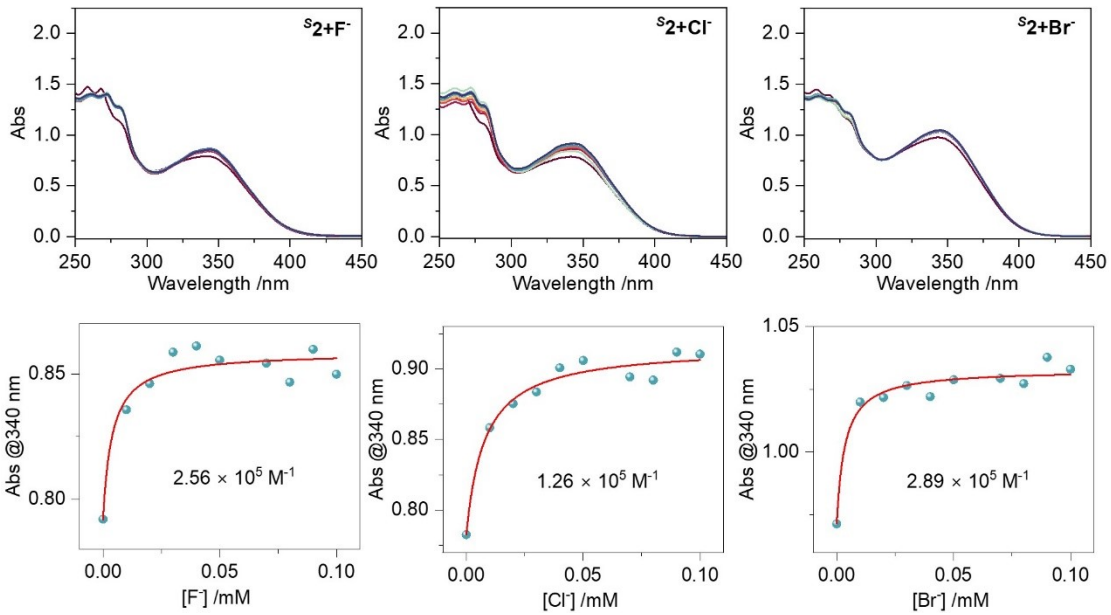

Figure S8. Absorption titration studies and the 1:1 fitted curve of ^{S}**2** (0.05 mM in THF) and F^-, Cl^- and Br^-.

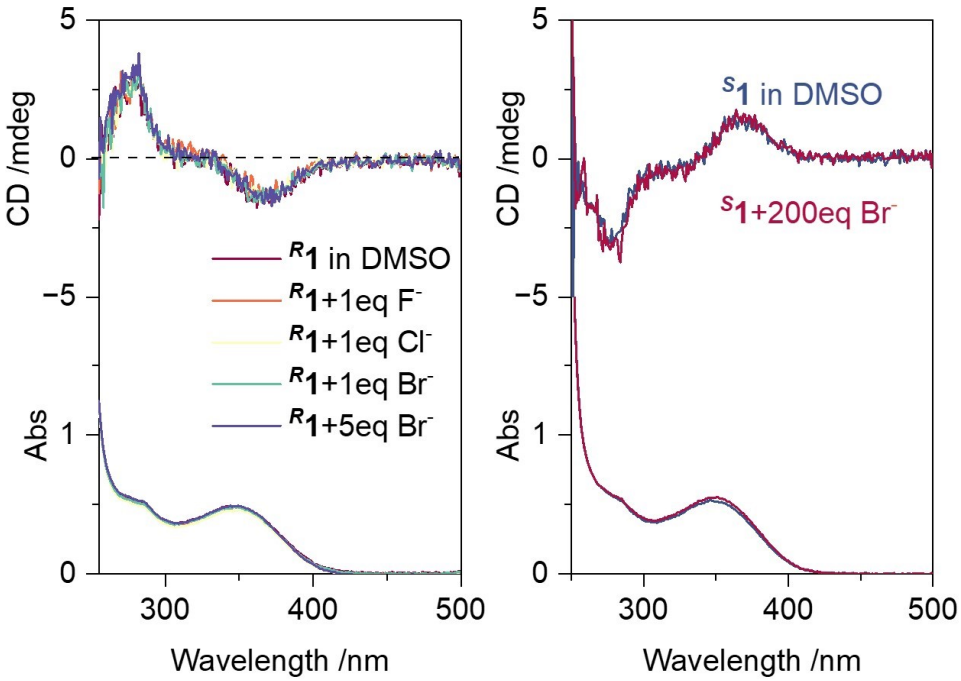

Figure S9. CD spectra changes of ^{R}**1** and ^{S}**1** (0.1 mM in DMSO) with increasing molar equiv. of F^-, Br^- and Cl^- respectively.

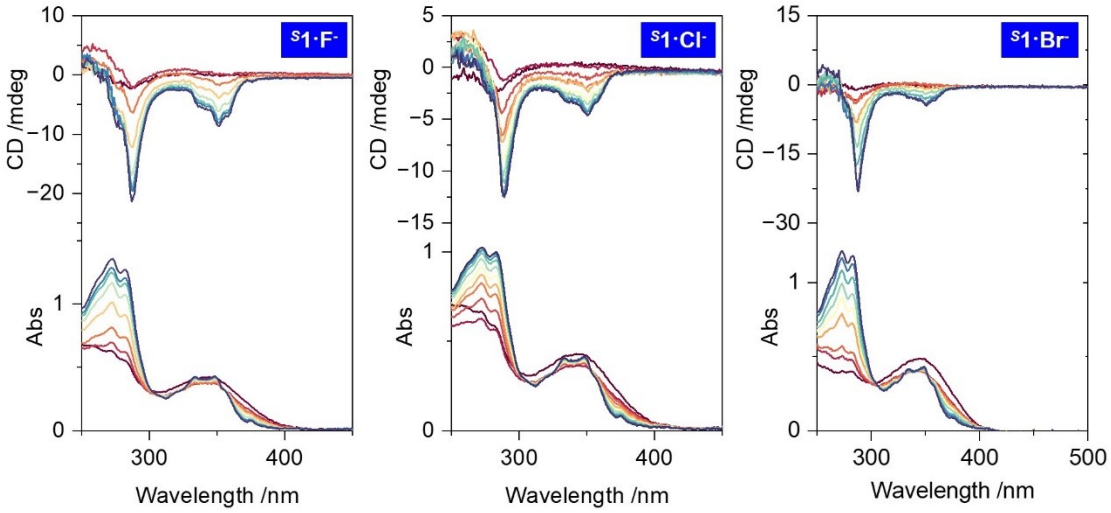

Figure S10. CD spectra of ^{S}**1·F**$^{-}$, ^{S}**1·Cl**$^{-}$ and ^{S}**1·Br**$^{-}$ (0.1 mM, 1:1 in THF) upon photo irradiation.

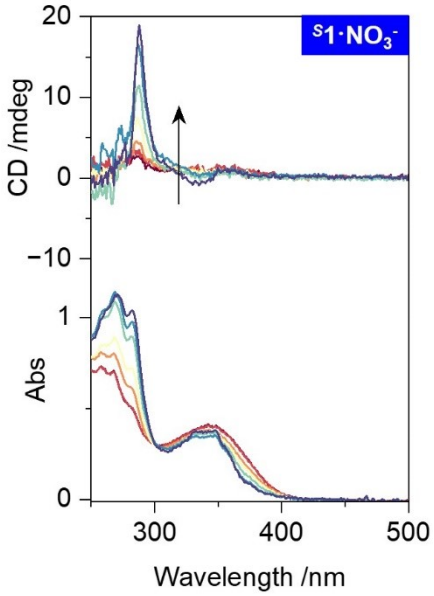

Figure S11. CD spectra of ^{S}**1·NO**$_3^-$ (0.1 mM, 1:1 in THF) upon photo irradiation.

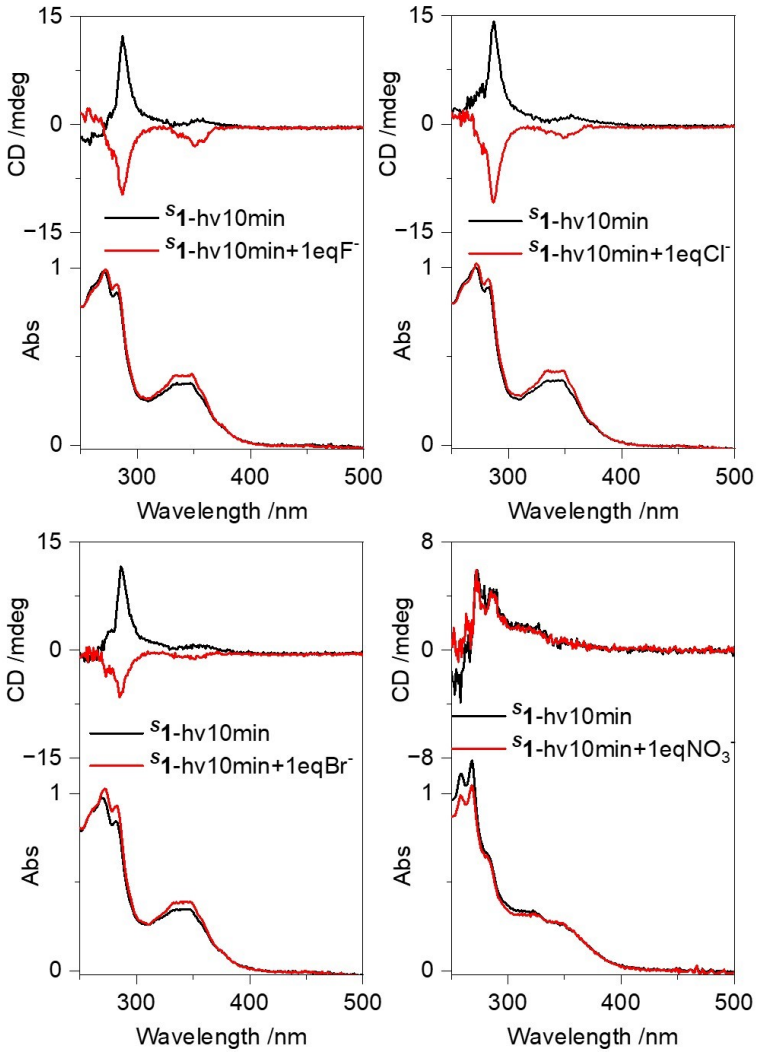

Figure S12. The comparison of CD spectra of ^{S}**1** after 10 min irradiation and the systems followed by the addition of anions (F^-, Cl^-, Br^- and NO_3^-).

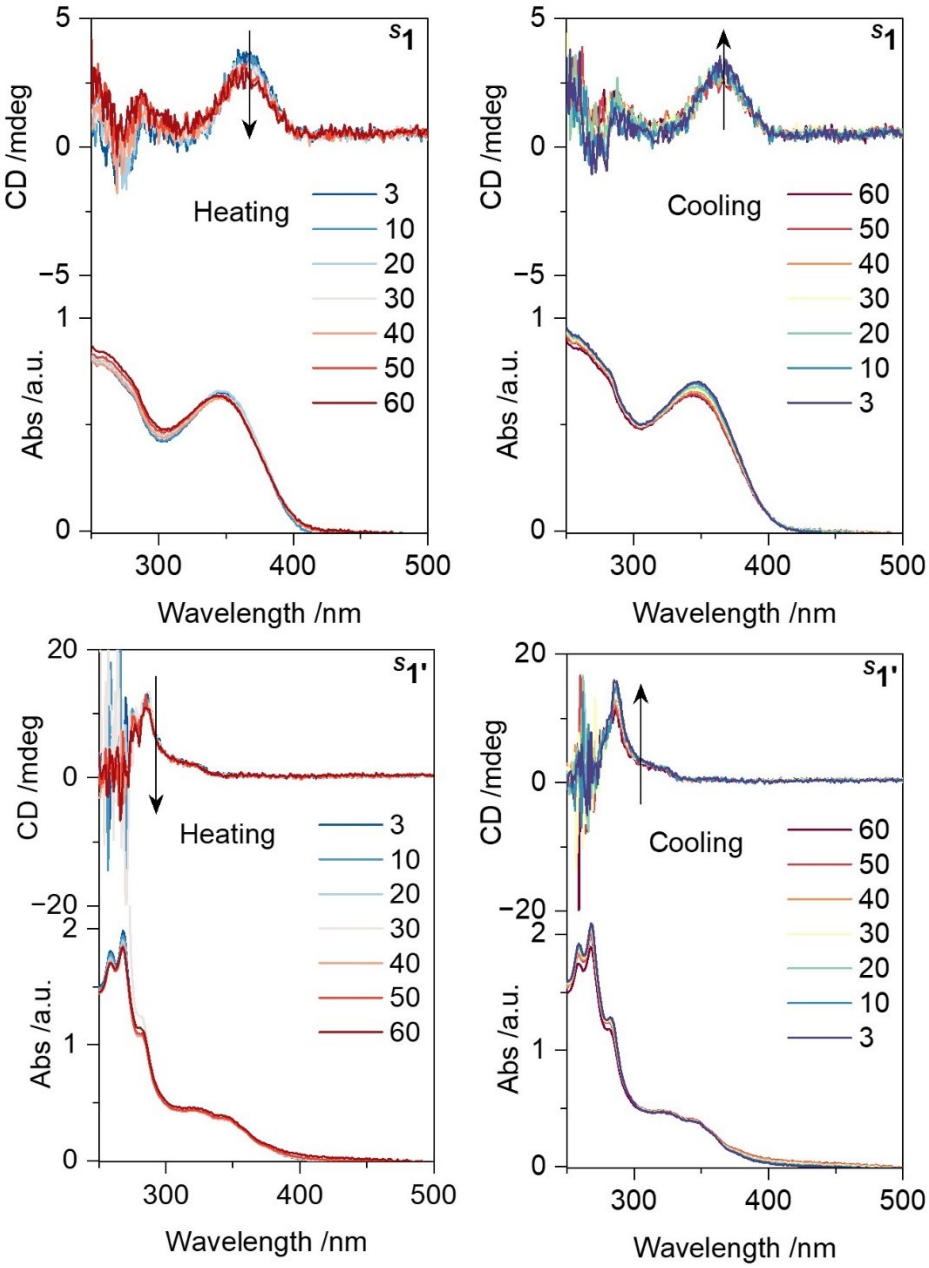

Figure S13. Variable temperature (VT)-CD spectra of ^{S}**1** and ^{S}**1′** in THF. $c = 2 \times 10^{-3}$ M.

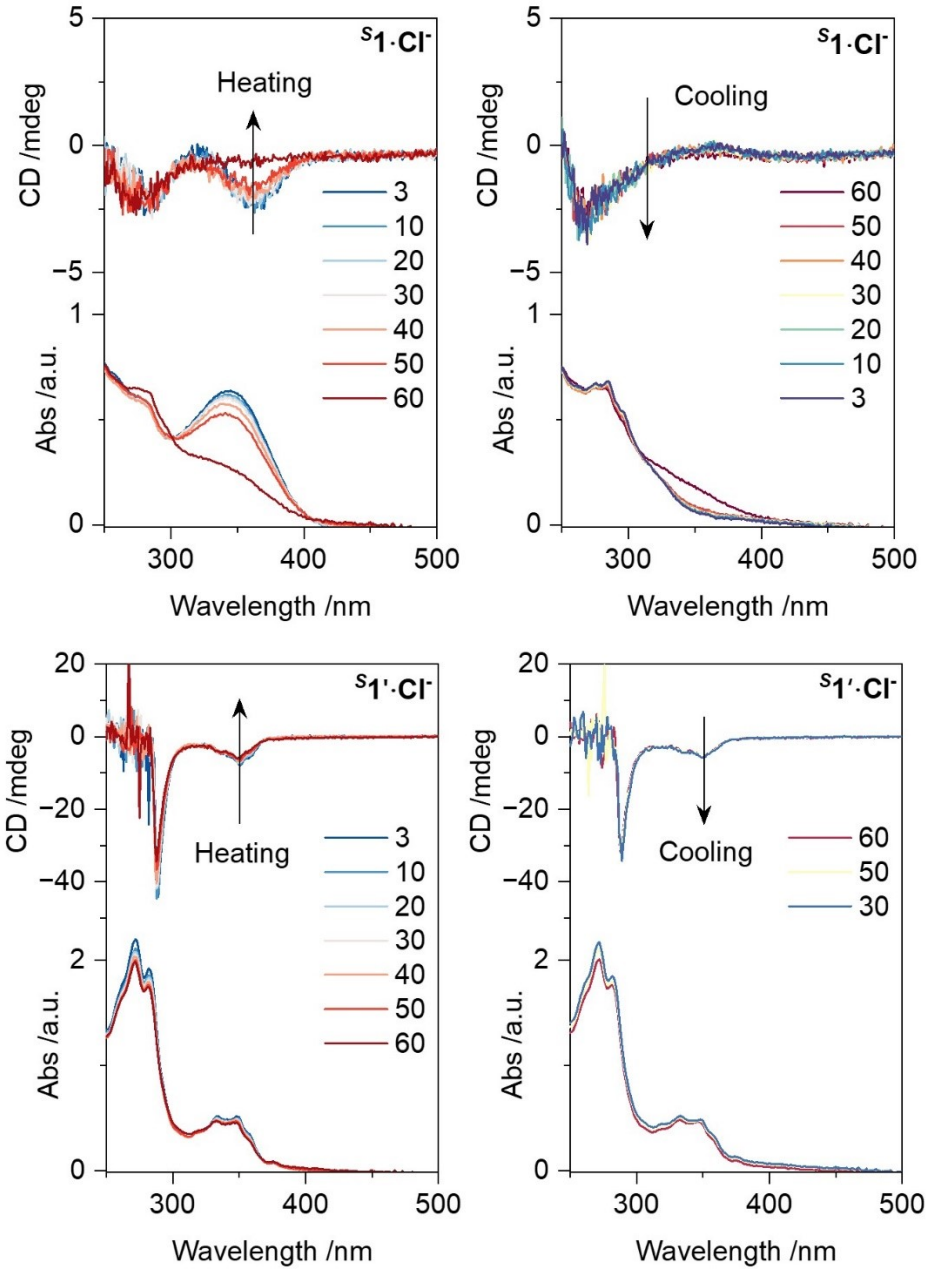

Figure S14. Variable temperature (VT)-CD spectra of ^{S}**1·Cl** and ^{S}**1′·Cl** in THF. c = 2 × 10^{-3} M.

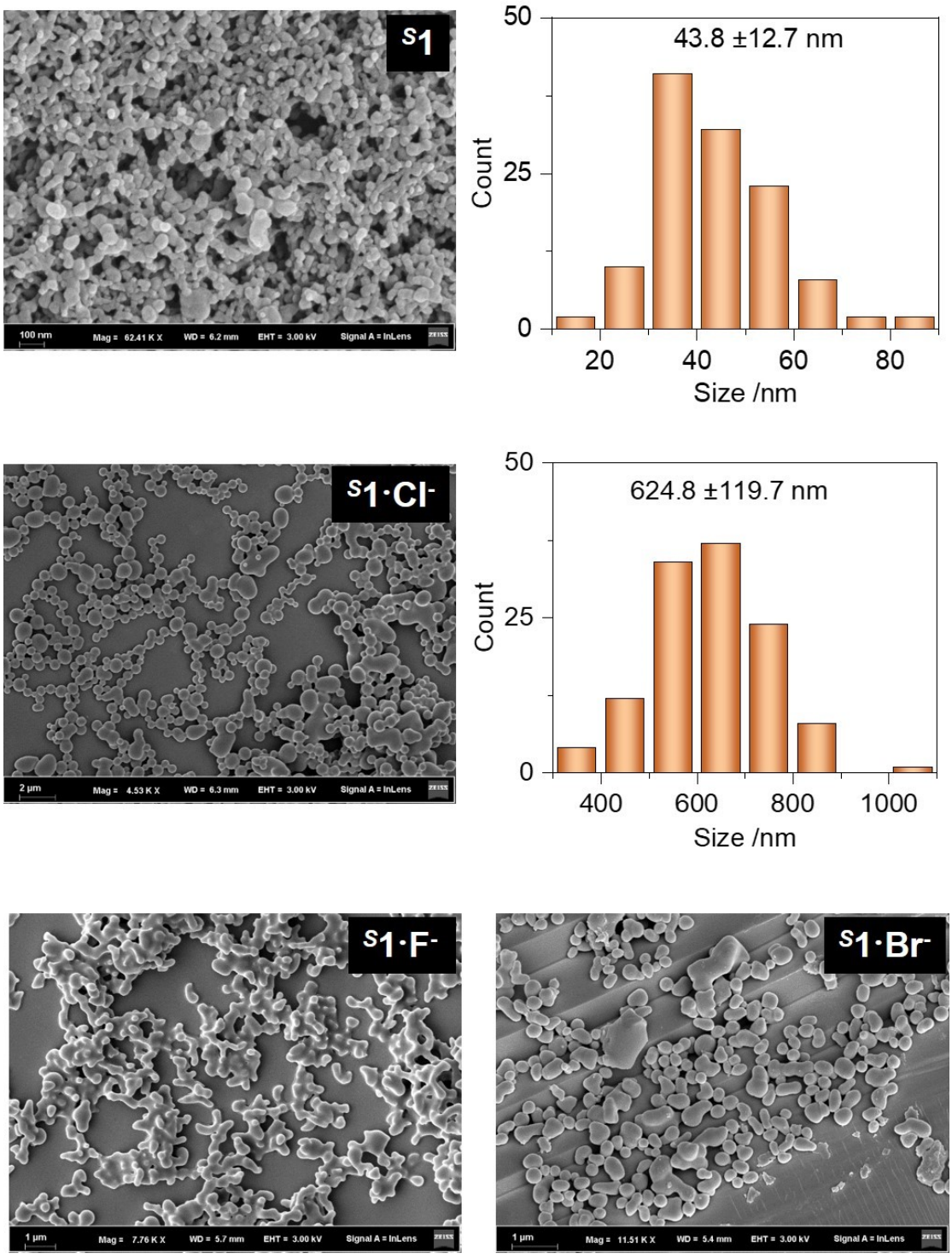

Figure S15. SEM images of ^{S}**1** and ^{S}**1**·**X**$^{-}$ (X^{-}= F^{-}, Cl^{-}, Br^{-}) and the statistics of particle size distribution.

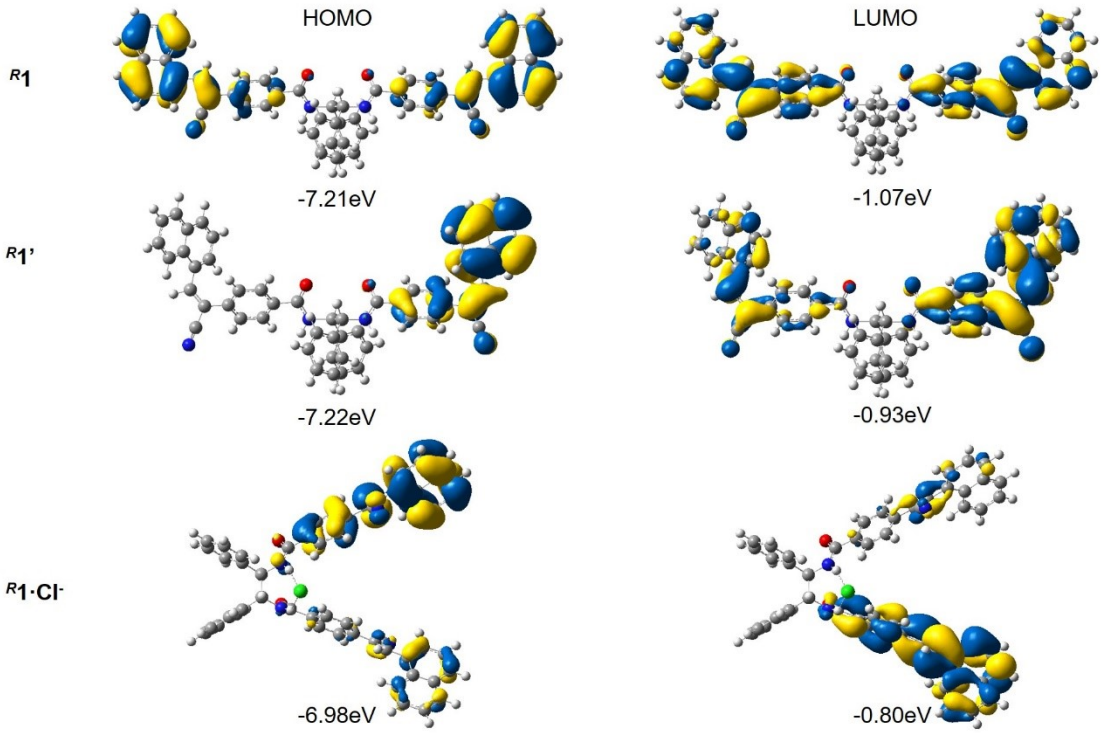

Figure S16 The calculated HOMOs and LUMOs for ^{R}**1**, ^{R}**1'** and ^{R}**1**·**Cl**$^{-}$.

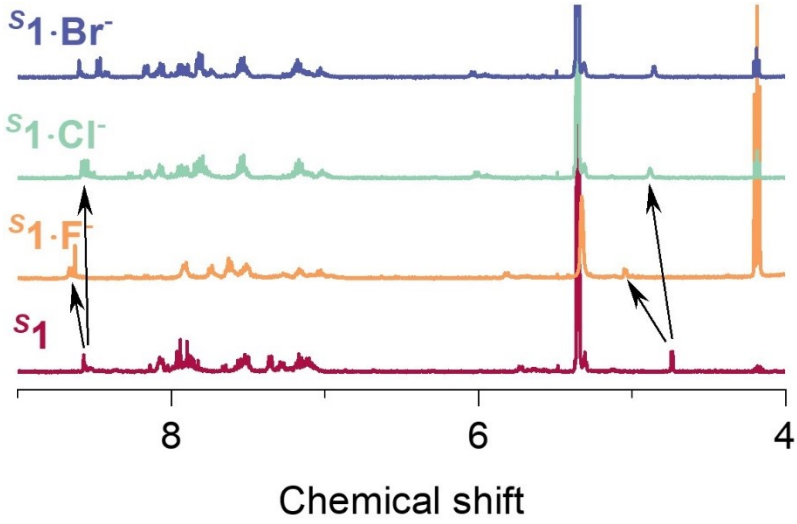

Figure S17. The ^{1}HNMR spectra in THF-d_8 for ^{S}**1**, ^{S}**1**·**F**$^{-}$, ^{S}**1**·**Cl**$^{-}$ and ^{S}**1**·**Br**$^{-}$. The concentration of ^{S}**1** is 5 × 10^{-3} M and all the molar ratios of ^{S}**1** and anions are 1:1.

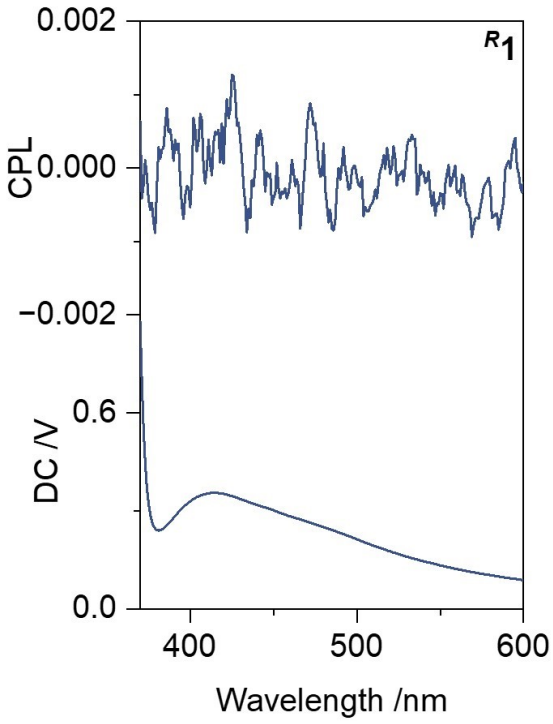

Figure S18. CPL spectra of ^{R}**1**. (λ_{ex} = 340 nm)

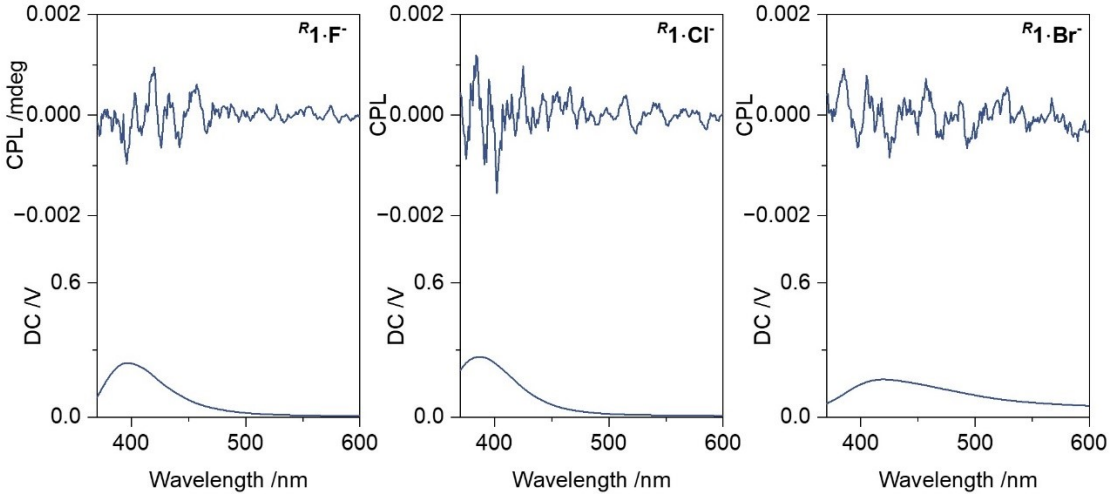

Figure S19. CPL spectra of ^{R}**1·X**$^{-}$ (X^{-}= F^{-}, Cl^{-}, Br^{-}). (λ_{ex} = 340 nm)

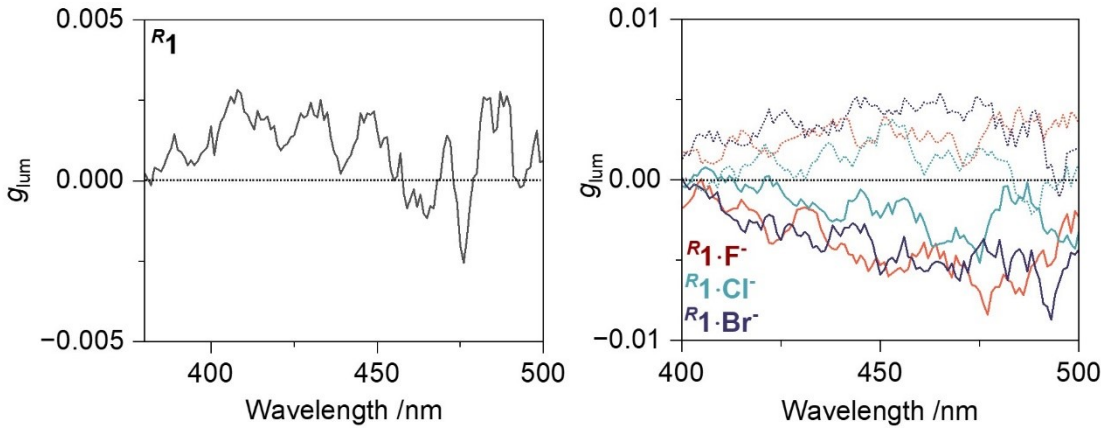

Figure S20. Dissymmetry factor g_{lum} of CPL spectra of ^{R}**1**, ^{S}**1·X**$^-$ and ^{S}**1·X**$^-$ (X$^-$= F$^-$, Cl$^-$, Br$^-$). (λ_{ex} = 340 nm)

III. Theoretical calculations

Calculations of ECD spectra[1]

For the compounds, the configuration was constructed by the skeleton extracted from the similar X-ray crystal structures and further modified by GaussView 6.0. Then, a whole conformational search was carried out by Spartan 14. Two main types of skeletons were found as shown in Figure S21, which were defined as “open” and “close” geometry, respectively. These structures were initially optimized at the CAMAB3LYP/6-311 G(d) level of the Gaussian 16 program to obtain a low-energy conformation, which did not alter the pristine geometries. Then, CAMB3LYP/6-311 G(d) level were utilized to calculate absorption/ECD spectra based on time-dependent density functional theory (TDDFT). For the other settings, nstates is set to 100, which represents the information of the 100 excited states with the lowest total computational energy. Moreover, IEFPCM is used as the implicit solvent model, and THF is used as the built-in solvent. Using the Gaussian output file, the UV-Vis and

ECD spectra can be plotted via GaussView 6.0.

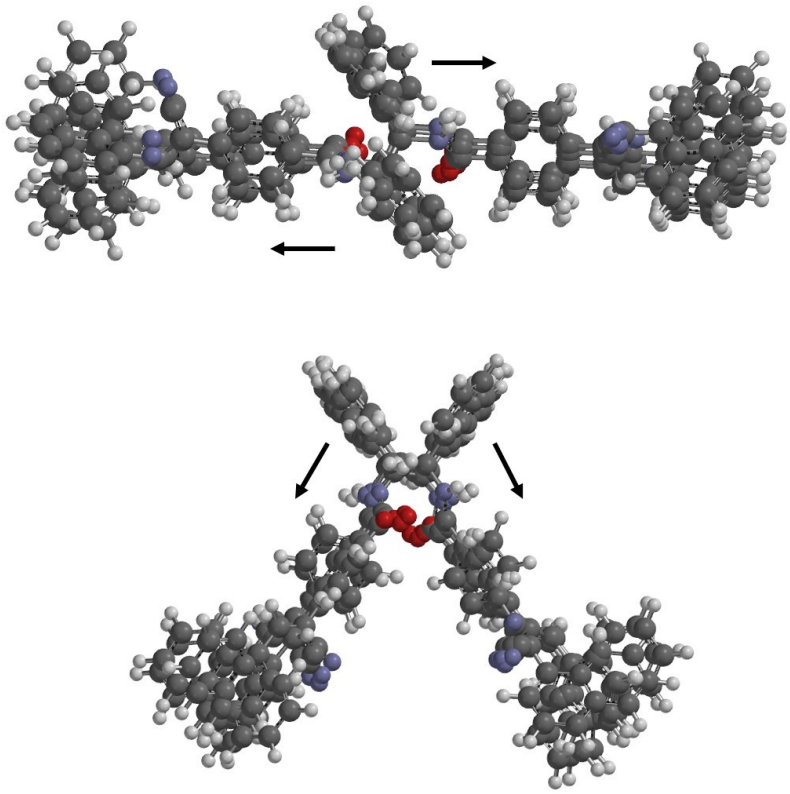

Figure S21. The "open" (top) and "close" (bottom) geometry found in the results of conformational search. Five dominant molecular structures were selected as examples to show the differences between the two geometries.

Calculations of binding energy

For the systems containing anions (in the case of Cl^-), we added Cl^- to the region around the N-H groups. Then, the optimition was conducted at the B3LYP/6-311 G(d) level. Whether ^{R}**1** or ^{R}**2**, multiple hydrogen bonds were identified between the compounds and Cl^- in the optimized structures. The host compound and Cl^- were divided into two groups to calculate the binding energy. In the output file, the corrected complexation energy were regarded as the results.

IV. Synthetic procedures and characterization

Synthesis and characterization

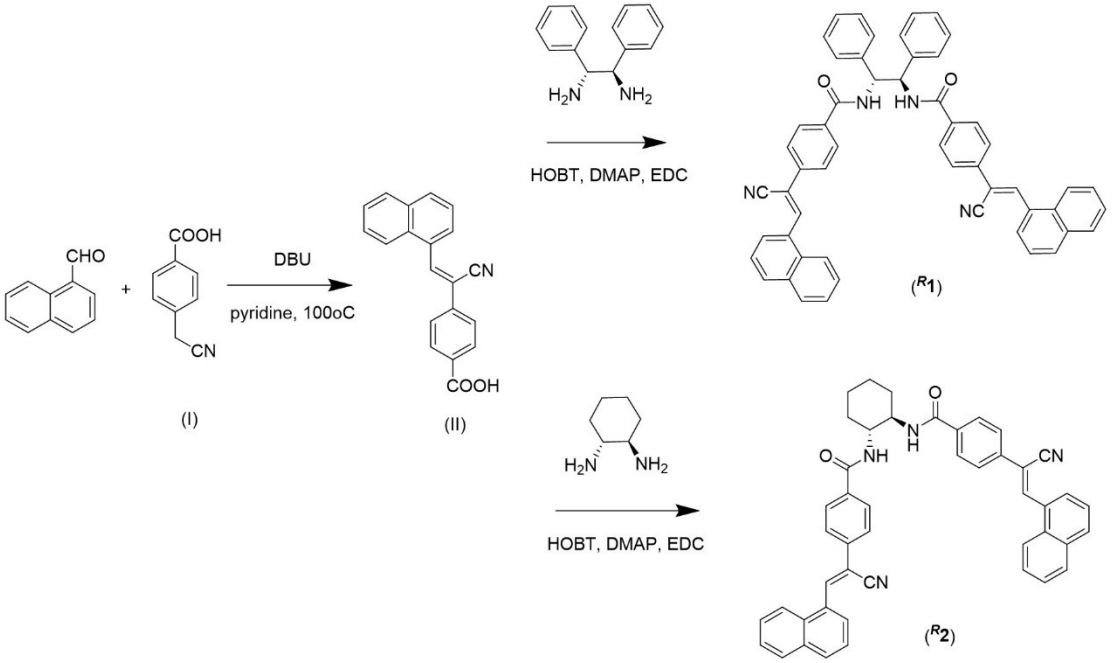

Scheme S1. The synthetic route of ***R*1** and ***R*2**.

The first step of the synthesis is according to the former report,[2] which is shown in Scheme S1. 4-(Cyanomethyl)benzoic acid (0.86 g, 5.0 mmol), 1-Naphthaldehyde (0.78 g, 5.0 mmol) were added in the 25 ml round-bottom flask and dissolved in pyridine (10 ml), followed by the addition of DBU (0.76 g, 5.0 mmol). The solution was refluxed overnight at 100 ^{o}C under the protection of N_2 atmosphere. The resulting solution was cooled and poured into H_2O (100ml). The mixture was extracted with 100 mL of CH_2Cl_2 three times, and the organic layer was subsequently washed with 100 mL of water. The organic solvent was concentrated under vacuum to obtain the crude product. The compound (**II)** obtained was purified by silica gel chromatography to get a faint yellow solid.

The second condensation reaction was accomplished by a common method used in our group.[3,4] Take ***R*1** as an example, compound (**II**) (300 mg, 0.5 mmol), (1R,2R)-Diphenylethane-1,2-diamine (106 mg, 0.25 mmol), HOBT (34 mg, 0.25 mmol), DMAP (31 mg, 0.25 mmol) and EDC (465 mg, 3.0 mmol) were dissolved in DMF (20 ml) and stirred overnight at room temperature. The solution obtained was added to

100 mL of water. The resulting mixture was extracted three times with 100 mL of CH_2Cl_2, and the organic layer was then washed with 100 mL of water. The organic layer was concentrated in vacuo and purified by silica gel chromatography to obtain the final product ***R*1**. Other compounds were successfully synthesized in the same way.

Compound (**II**): Faint yellow solid. Yield: 70%. ^{1}H NMR (500 MHz, DMSO-d_6) δ 13.21 (s, 1H), 8.89 (s, 1H), 8.23 – 8.18 (m, 1H), 8.17 – 8.08 (m, 3H), 8.07 – 7.94 (m, 4H), 7.71 – 7.60 (m, 3H). ^{13}C NMR (101 MHz, DMSO-d_6) δ 167.21, 143.97, 137.82, 133.52, 131.84, 131.76, 131.47, 131.35, 130.55, 130.29, 129.32, 129.14, 127.65, 127.46, 127.22, 126.88, 125.97, 124.74, 117.81, 114.30. HRMS (ESI) m/z $[M+H]^+$, calcd for $C_{20}H_{13}NO_2$, 299.0946; found 298.0873.

***R*1**: Yellow solid. Yield: 95%. ^{1}H NMR (500 MHz, DMSO-d_6) δ 9.34 – 9.19 (m, 1H), 8.82 (d, J = 5.0 Hz, 1H), 8.18 – 7.92 (m, 6H), 7.80 – 7.47 (m, 4H), 7.43 – 7.09 (m, 6H), 5.77 – 5.67 (m, 1H). ^{13}C NMR (101 MHz, DMSO) δ 166.01, 143.42, 141.05, 136.46, 135.70, 135.63, 133.52, 131.79, 131.45, 131.25, 129.51, 129.14, 129.06, 128.57, 128.45, 128.00, 127.89, 127.62, 127.41, 127.20, 126.65, 125.97, 124.71, 117.86, 115.41, 114.34, 58.12, 57.96. HRMS (ESI) m/z $[M+H]^+$, calcd for $C_{54}H_{38}N_4O_2$, 774.2995; found 775.3082.

***R*2**: Yellow solid. Yield: 96%. ^{1}H NMR (500 MHz, DMSO-d_6) δ 8.81 (d, J = 4.4 Hz, 2H), 8.46 (d, J = 7.6 Hz, 2H), 8.22 – 8.15 (m, 2H), 8.09 (d, J = 8.2 Hz, 2H), 8.06 – 7.99 (m, 4H), 7.97 – 7.89 (m, 6H), 7.64 (qdt, J = 15.4, 10.7, 5.0 Hz, 8H), 4.03 (t, J = 9.1 Hz, 2H), 1.94 (d, J = 12.8 Hz, 2H), 1.79 (s, 2H), 0.91 – 0.72 (m, 4H). ^{13}C NMR (101 MHz, DMSO) δ 135.00, 132.43, 130.76, 130.37, 130.07, 128.03, 127.41, 127.33, 127.14, 126.31, 126.10, 125.39, 124.88, 123.68, 116.80, 113.34, 52.46, 31.09, 28.24, 25.73, 24.44, 21.76. HRMS (ESI) m/z $[M+H]^+$, calcd for $C_{46}H_{36}N_4O_2$, 676.2838; found 675.6733.

^{1}H NMR and ^{13}C NMR and HRMS spectra of synthesized compounds

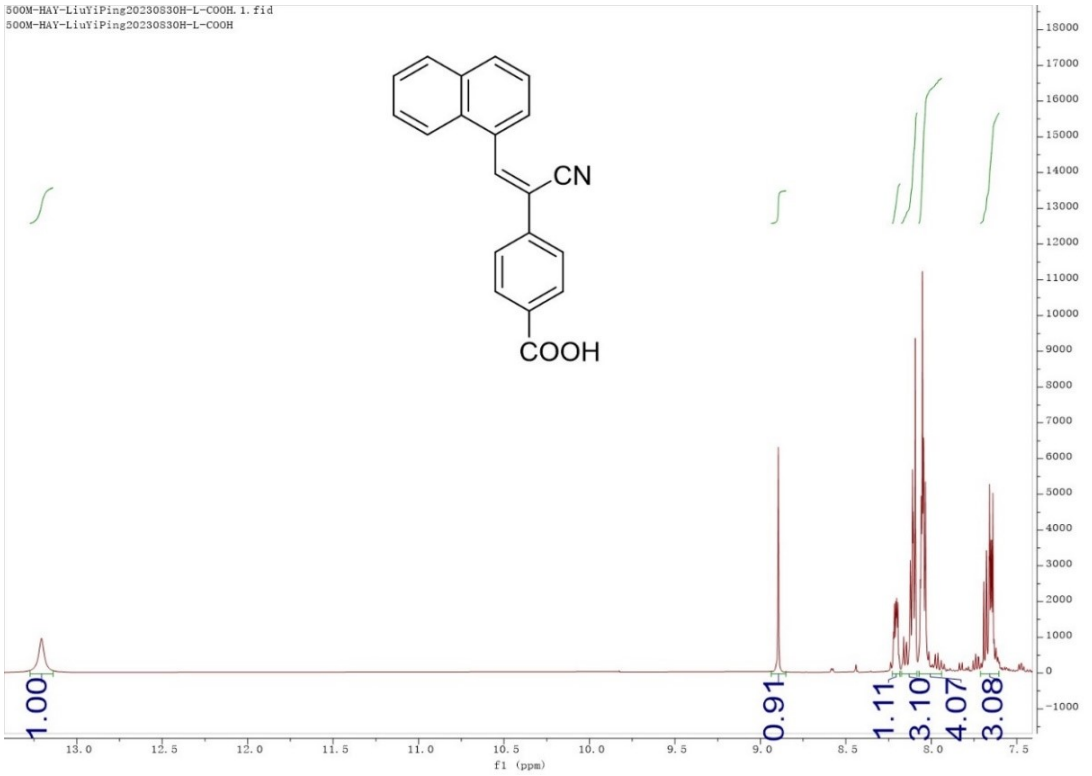

Figure S22. ^{1}H NMR of compound (**II**).

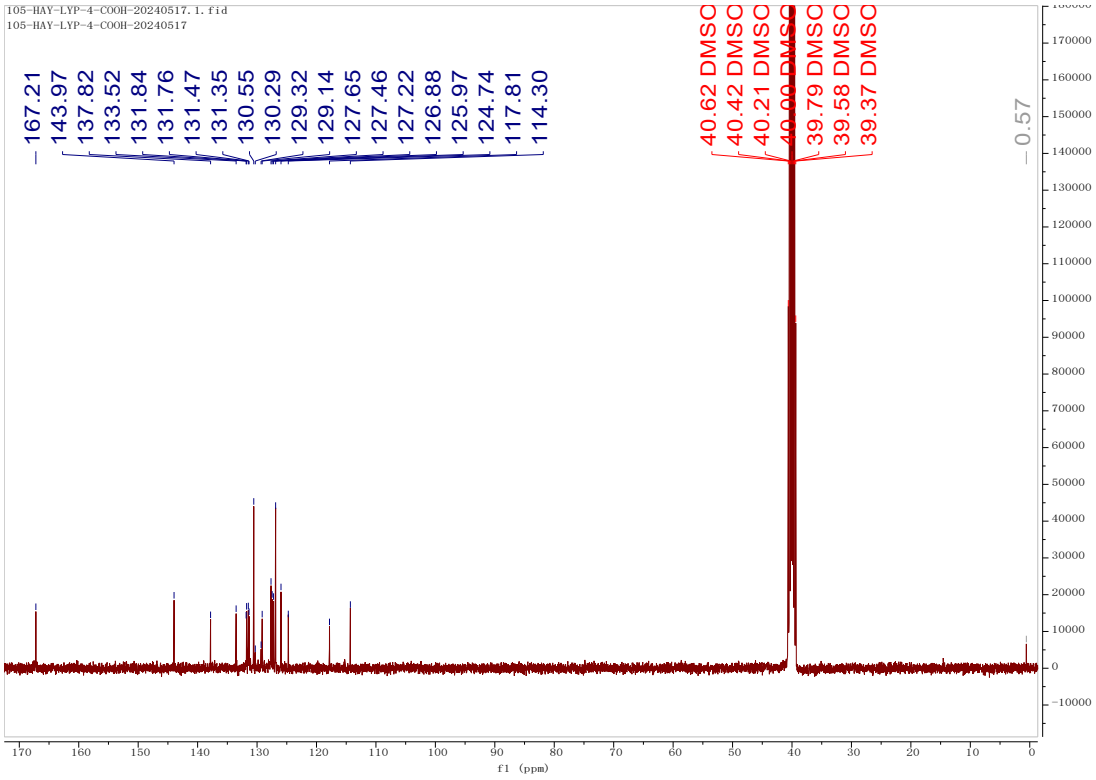

Figure S23. ^{13}C NMR of compound (**II**).

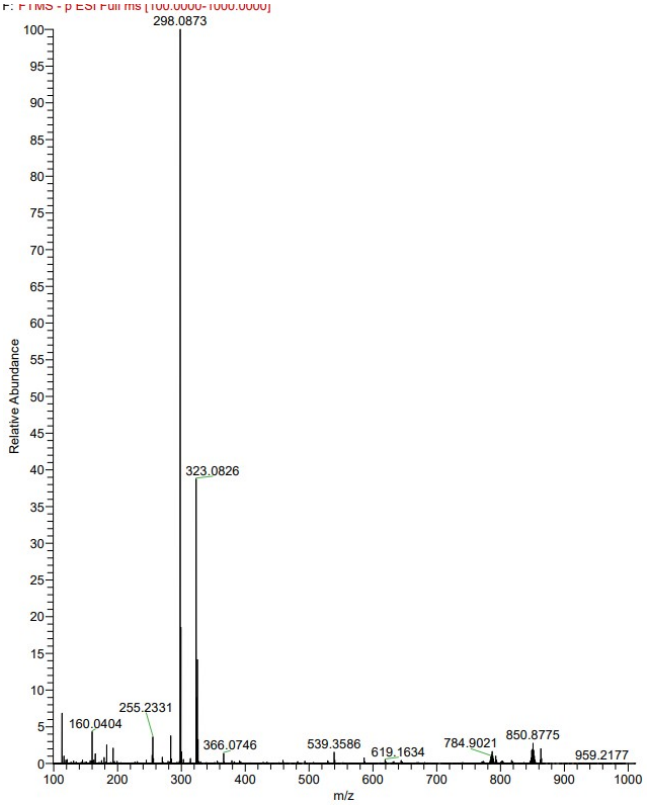

Figure S24. HRMS of compound (**II**).

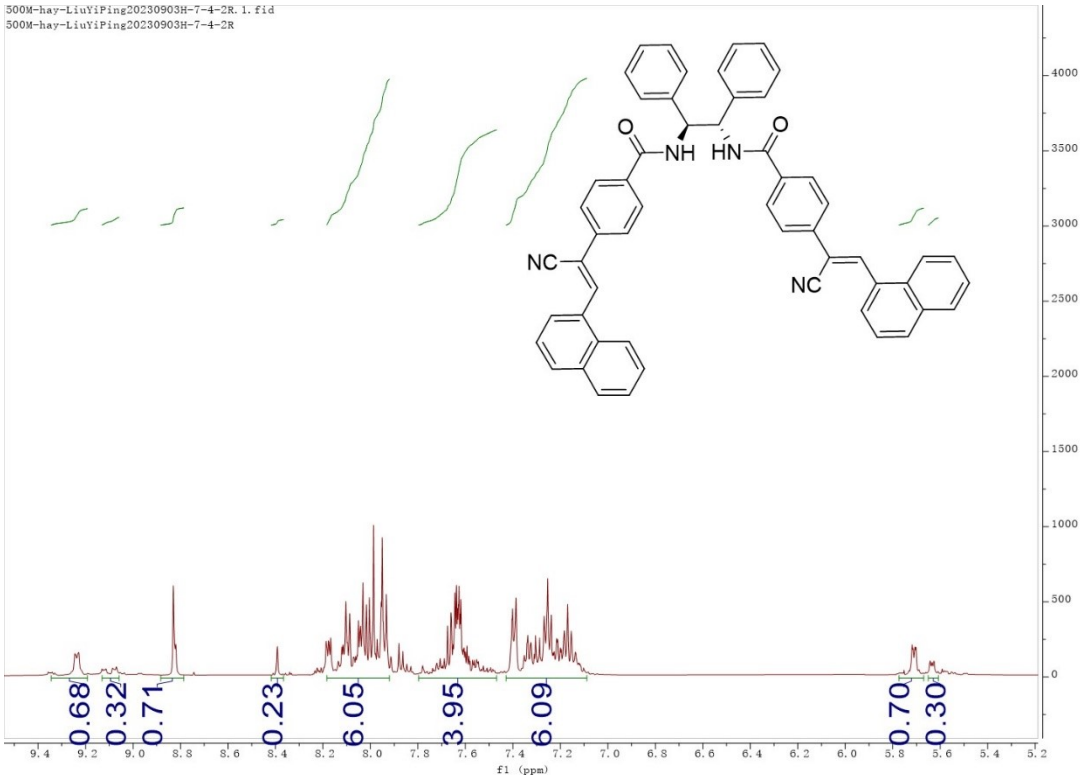

Figure S25. ^{1}H NMR of ***R*1**.

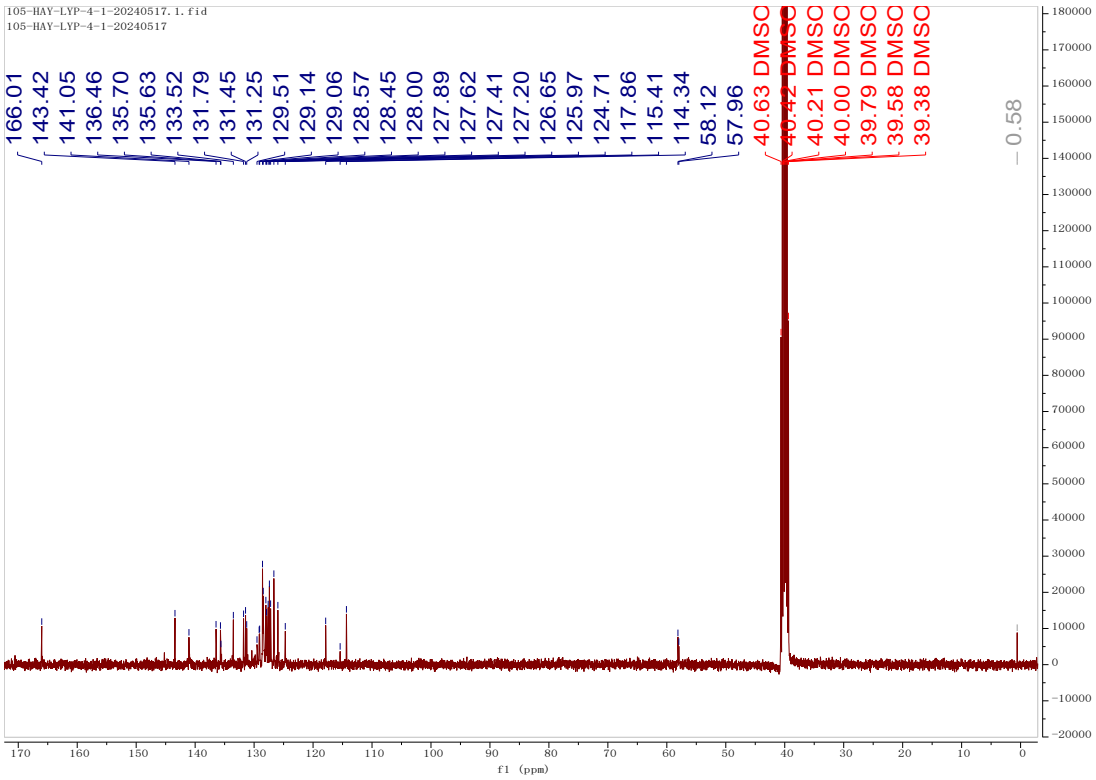

Figure S26. ^{13}C NMR of ***R*1**.

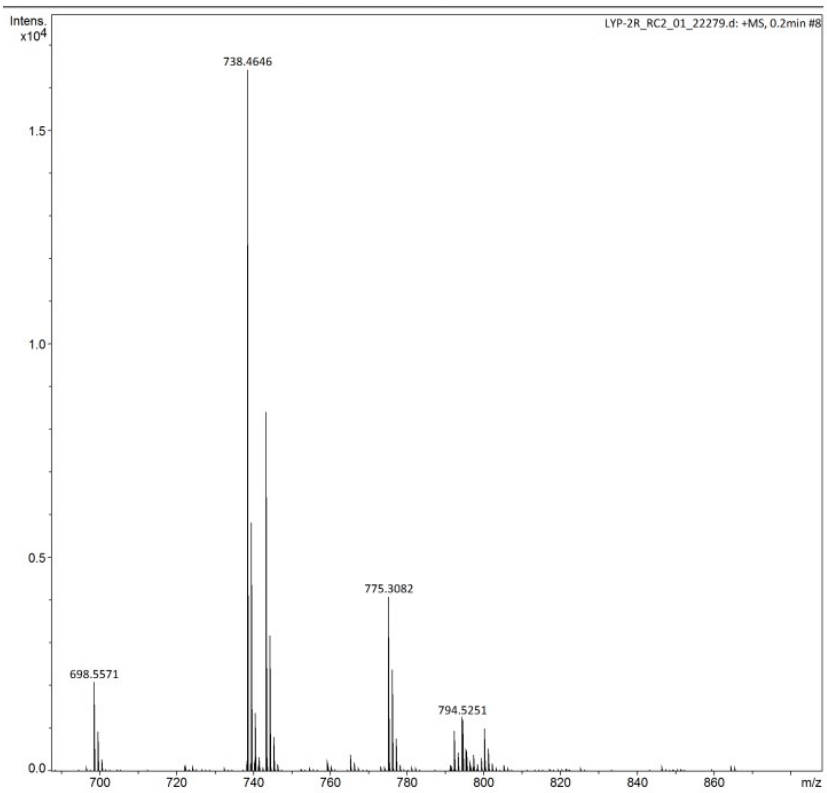

Figure S27. HRMS of ***R*1**.

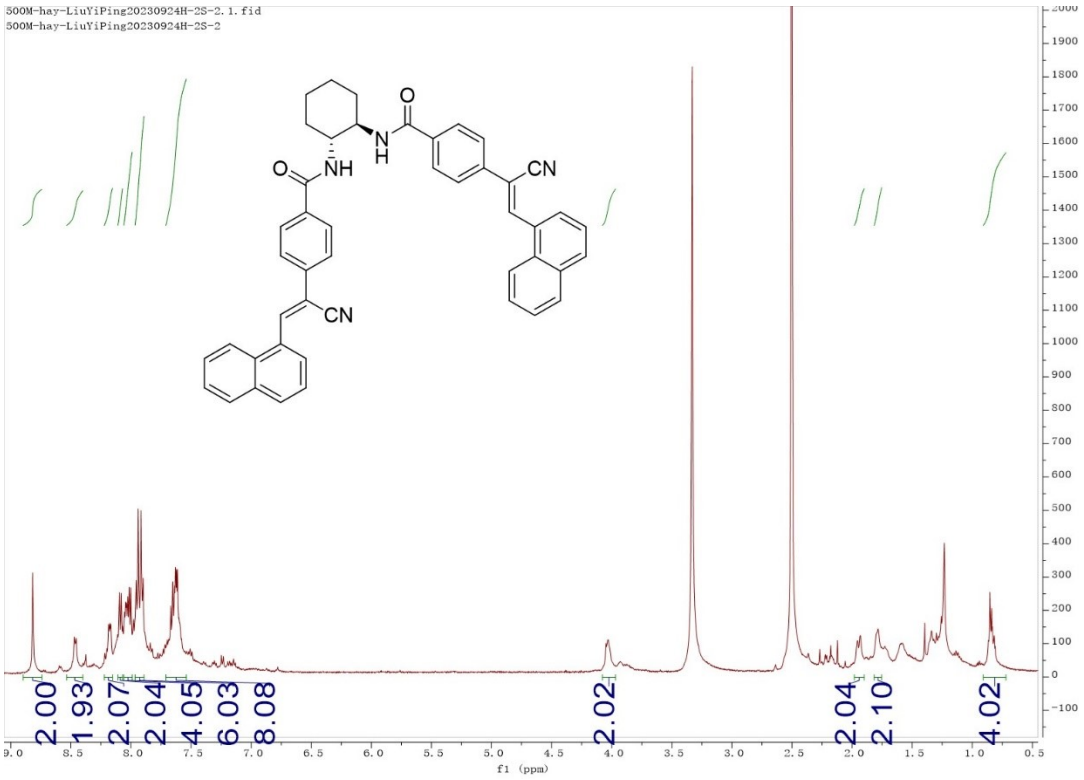

Figure S28. ^{1}H NMR of ***R*2**.

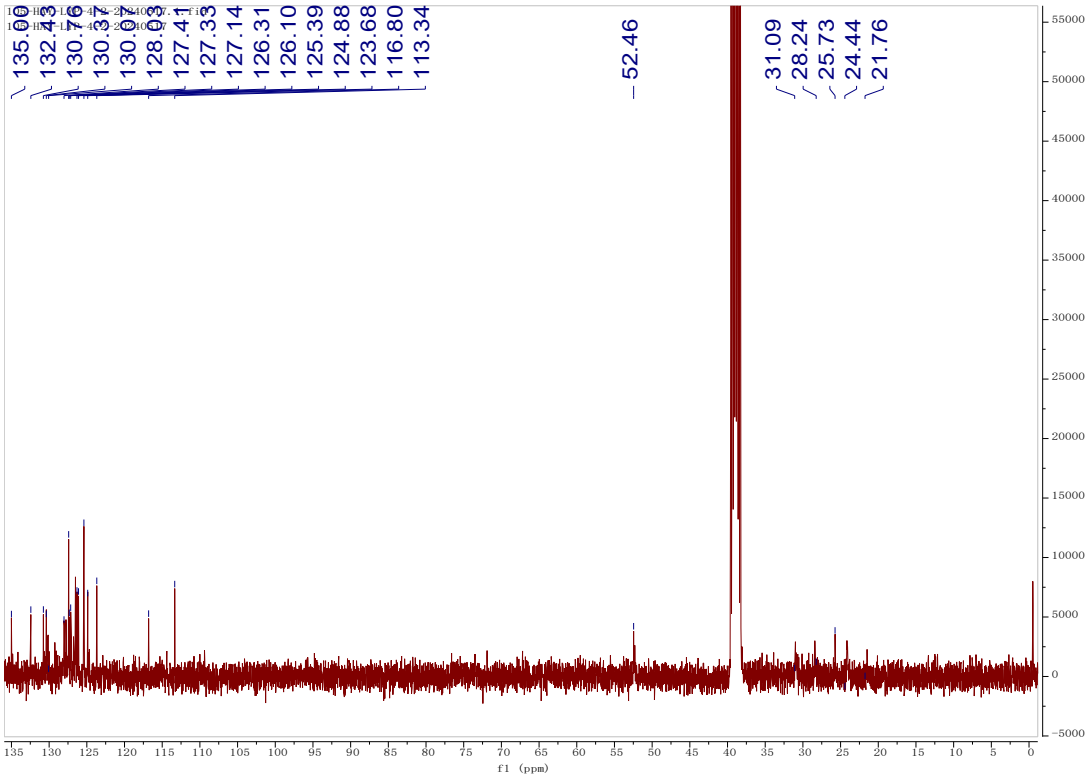

Figure S29. ^{13}C NMR of ***R*2**.

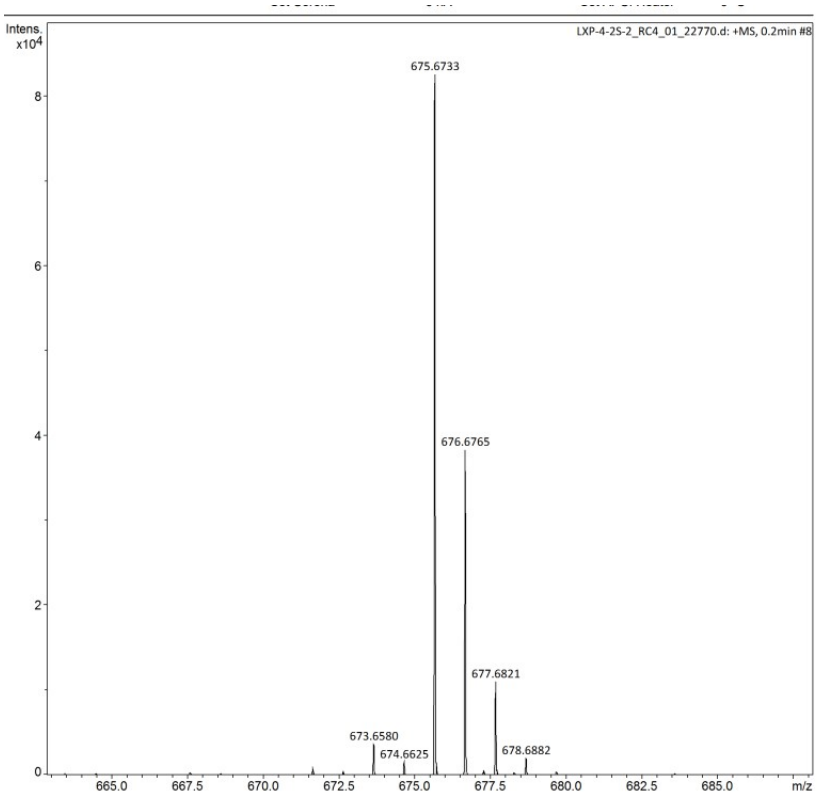

Figure S30. HRMS of ***R*2**.

V. Ultraviolet titration

The ultraviolet titration curves were fitted by the formula [S5,S6]:

$$\varepsilon_{obs} = \varepsilon_h + \frac{\varepsilon_{hg} - \varepsilon_h}{2c_h^0}(c_h^0 + c_g^0 + \frac{1}{K_a} \pm \sqrt{\left(c_h^0 + c_g^0 + \frac{1}{K_a}\right)^2 - 4c_h^0 c_g^0})$$

where ε_h, ε_{hg} and ε_{obs} as extinction coefficients at a given wavelength of the free compound, the compound-anion complex and the measured extinction coefficient, c_h^0 and c_g^0 as total concentrations of the compound and the anion and Ka as binding constant. Ka was treated as shared variable.

The detailed information was concluded in Table S1.

Table S1. The fitting parameters of the ultraviolet titration for compounds with anions.

Cmpd	Anions	K_a /M^{-1}	R-square
1	F^-	$3.5 \pm 0.9 \times 10^4$	0.97
	Cl^-	$7.6 \pm 1.3 \times 10^4$	0.98
	Br^-	$9.6 \pm 2.5 \times 10^4$	0.96

	F^-	$2.6 \pm 1.4 \times 10^5$	0.93
2	Cl-	$1.3 \pm 0.3 \times 10^5$	0.97
	Br-	$2.9 \pm 1.1 \times 10^5$	0.96

VI. Supplementary references

S1. Gaussian 16, Revision B.01, M. J. Frisch, G. W. Trucks, H. B. Schlegel, G. E. Scuseria, M. A. Robb, J. R. Cheeseman, G. Scalmani, V. Barone, G. A. Petersson, H. Nakatsuji, X. Li, M. Caricato, A. V. Marenich, J. Bloino, B. G. Janesko, R. Gomperts, B. Mennucci, H. P. Hratchian, J. V. Ortiz, A. F. Izmaylov, J. L. Sonnenberg, D. Williams-Young, F. Ding, F. Lipparini, F. Egidi, J. Goings, B. Peng, A. Petrone, T. Henderson, D. Ranasinghe, V. G. Zakrzewski, J. Gao, N. Rega, G. Zheng, W. Liang, M. Hada, M. Ehara, K. Toyota, R. Fukuda, J. Hasegawa, M. Ishida, T. Nakajima, Y. Honda, O. Kitao, H. Nakai, T. Vreven, K. Throssell, J. A. Montgomery, Jr., J. E. Peralta, F. Ogliaro, M. J. Bearpark, J. J. Heyd, E. N. Brothers, K. N. Kudin, V. N. Staroverov, T. A. Keith, R. Kobayashi, J. Normand, K. Raghavachari, A. P. Rendell, J. C. Burant, S. S. Iyengar, J. Tomasi, M. Cossi, J. M. Millam, M. Klene, C. Adamo, R. Cammi, J. W. Ochterski, R. L. Martin, K. Morokuma, O. Farkas, J. B. Foresman, and D. J. Fox, Gaussian, Inc., Wallingford CT, 2016.

S2. L. Zhu, C. Y. Ang, X. Li, K. T. Nguyen, S. Y. Tan, H. Ågren and Y. Zhao, *Adv. Mater.,* 2012, **24**, 4020– 4024.

S3. Z. Wang, A. Hao and P. Xing, *Chem. Mater*., 2022, **34**, 1302–1314.

S4. Z. Wang, A. Hao and P. Xing, *Angew. Chem. Int. Ed.,* 2020, **59**, 11556-11565.

S5. P. Thordarson, *Chem. Soc. Rev*., 2011, **40**, 1305−1323.

S6. M. Sapotta, A. Hofmann, D. Bialas and F. Würthner, *Angew. Chem., Int. Ed.*, 2019, **58**, 3516-3520.